Rule-Based Predictive Control for Battery Scheduling in Microgrids under Power Generation and Load Uncertainties

M. Kaheni, *Member, IEEE*, J. Fu *Member, IEEE*, A. V. Papadopoulos *Senior Member, IEEE*

***Abstract*—This paper addresses the control of the state of charge (SoC) of a Battery Energy Storage System (BESS) in a microgrid, considering uncertainties in load and Renewable Energy Sources (RES) generated power estimations. To achieve this objective, we propose RubPC, a novel rule-based Model Predictive Control (MPC). We partition the feasible operation space of the microgrid into two subzones, referred to as the *white* and *yellow* zones. The yellow zone represents the boundary space between the feasible and unfeasible operation spaces. In RubPC, we initially implement MPC on a predefined optimization window to determine the optimal SoC of the BESS, aiming to keep the microgrid within the *white* zone. Noting that mismatches between estimated and actual load and generated power may lead to constraint violations, we introduce a rule-based controller as a supervisory control. This controller monitors the microgrid's state, and if the microgrid enters the *yellow* zone, it adjusts the control to maintain the microgrid within the *white* zone. We validate our proposed method by simulating it using data from an electrified quarry site in Sweden.**

***Note to Practitioners*—Optimizing the charge and discharge schedule of BESSs in microgrids offers a promising avenue for substantial economic and technical benefits. However, the successful realization of these benefits hinges on accurately estimating and aligning the values of load and RES-generated power. In industries, the consequences of mismatches between these estimates and actual values can translate into unexpected costs that may outweigh the anticipated economic benefits of BESS's optimal charge and discharge schedule. This paper underscores the critical importance of addressing this concern to ensure the viability of BESS applications in various industries. To tackle this challenge, we present RubPC, an innovative Rule-Based MPC framework. Unlike conventional approaches, RubPC is specifically designed to effectively handle discrepancies between estimated and actual values, thereby preventing potential constraint violations. Our aim is to offer practitioners a robust solution that not only brings economic benefits but also ensures their safe and reliable operation.**

***Index Terms*—Battery Energy Storage System (BESS), Demand-side Management (DSM), Model Predictive Control (MPC), Optimization, Rule-based Control.**

I. Introduction

This work was supported by the Swedish Agency for Innovation Systems (Vinnova) with grant "GREENER: Intelligent energy management in connected construction sites" n. 2019-05877, and by the Knowledge Foundation (KKS) with grants "Safe and Secure Adaptive Collaborative Systems (SACSys)", n. 20190021, and "Mälardalen University Automation Research Center (MARC)", n. 20240011.

M. Kaheni and A. V. Papadopoulos are affiliated with Mälardalen University, Västerås, Sweden. e-mail: mojtaba.kaheni@mdu.se, alessandro.papadopoulos@mdu.se.

J. Fu is affiliated with The Swedish National Road and Transport Research Institute (VTI), Sweden. e-mail: jiali.fu@vti.se.

Nomenclature

q	Total number of time samples
$\mathbf{c}_{sell}$	Electrical energy selling tariff
$\mathbf{p}_{sell}$	Power sold to the grid
$\mathbf{c}_{buy}$	Electrical energy purchasing tariff
$\mathbf{p}_{buy}$	Power bought from the grid
$\mathbf{c}_a$	Degradation cost of battery
$\mathcal{X}$	Feasible space of decision variable
Ω	A set with cardinality of possible constraints set
ω	A member of Ω
Q	Capacity of BESS
ζ	State of charge (SoC)
${\mathbf{p}_b}^+$	Charging power of BESS
${\mathbf{p}_b}^-$	Discharging power of BESS
$\mathbf{p}_{b_l^-}$	Locally consumed discharging power of BESS
$\mathbf{p}_{b_s^-}$	Discharging power of BESS sold to the grid
η	Round trip efficiency of BESS
$\mathbf{p}_g$	Total generated power in industrial load
$\mathbf{p}_{g_l}$	Locally consumed generated power
$\mathbf{p}_{g_s}$	Power locally generated sold to the gird
${\mathbf{p}_b}^{\max}$	Max. allowable charging power of BESS
${\mathbf{p}_b}^{\min}$	Min. allowable discharging power of BESS
Δt	Sampling time
$\zeta^{\max}$	Max. allowable SoC of BESS
$\zeta^{\min}$	Min. allowable SoC of BESS
m^1	Slope of the power limit on discharge
m^2	Slope of the power limit on charge
b^1	Intercept of the power limit on discharge
b^2	Intercept of the power limit on charge
$\mathbf{p}_l$	Local power consumption of industrial load
$\mathbf{p}_l^{\max}$	Max. allowable power exchange
α	Safety margin of the SoC
β	Safety margin of the power exchange limit
T	Length of MPC optimization window
T_c	Length of control horizon
$(.)^\intercal$	Matrix transpose
$\lvert . \rvert$	Set cardinality

THE increasing emphasis on transitioning towards sustainable and eco-friendly practices in industries has spurred the adoption of Renewable Energy Sources (RESs) such as wind farms and solar panels. However, the intermittent and unpredictable nature of RESs necessitates the widespread implementation of controllable energy storage systems. Battery Energy Storage Systems (BESS) stand out as a vital solution for achieving objectives like smoothing load flow [1], [2], peak shaving [3], [4], or tracking a desired load [5]. However, on the customer side, the most appealing objective is optimizing return on investment by integrating these BESS units with existing microgrids [6]–[8]. Consequently, a compelling practical question arises: How can the State of Charge (SoC) of BESS be effectively controlled to minimize energy costs for its owners?

In theory, addressing this question appears straightforward, as it involves solving a constraint optimization problem that relies on accurate estimations of RES generation and demand across different time intervals, i.e.,

$$\begin{array}{ll} \text{minimize} & -\mathbf{c}_{sell}^{\intercal}\mathbf{p}_{sell} + \mathbf{c}_{buy}^{\intercal}\mathbf{p}_{buy} - \mathbf{c}_{a}^{\intercal}(\mathbf{p}_{b_l}^{-} + \mathbf{p}_{b_s}^{-}) \\ \text{subject to:} & \left[\mathbf{p}_{b}^{+}, \mathbf{p}_{b_l}^{-}, \mathbf{p}_{b_s}^{-}, \mathbf{p}_{g_l}, \mathbf{p}_{g_s}\right] \in \mathcal{X} \end{array}, \tag{1}$$

where the vectors $\mathbf{c}_{buy}, \mathbf{c}_{sell} \in \mathbb{R}_+^q$ represent purchase and sell tariffs at q sampled times within the optimization window, and $\mathbf{c}_a \in \mathbb{R}_+^q$ is the degradation cost of battery [9]. $\mathbf{p}_b^{+} \in \mathbb{R}_+^q$ represents charging power of BESS at q sampled times, $\mathbf{p}_{b_l}^{-} \in \mathbb{R}_-^q$ represents the power locally consumed during a discharge and $\mathbf{p}_{b_s}^{-} \in \mathbb{R}_-^q$ is the power sold to the grid during a discharge, and finally, $\mathbf{p}_{g_l} \in \mathbb{R}_-^q$ and $\mathbf{p}_{g_s} \in \mathbb{R}_-^q$ represent local consumption of the RES generated power and power which is sold to the grid from RES generated power, respectively. $\mathbf{p}_{sell}, \mathbf{p}_{buy} \in \mathbb{R}_+^q$ correspond to the sold and bought power at time samples, which are indeed function of decision variables, i.e. $\mathbf{p}_{sell} = f_s(\mathbf{p}_{b_s}^{-}, \mathbf{p}_{g_s})$ and $\mathbf{p}_{buy} = f_b(\mathbf{p}_b^{+}, \mathbf{p}_{b_l}^{-}, \mathbf{p}_{g_l})$. Finally, The decision variable should remain within the feasible space $\mathcal{X}$, defined by the constraints. However, inaccuracies in RES generation and load estimations can lead to results that violate crucial constraints. The uncertainties in RES generation and load would change the feasible space of the decision variable in (1). Therefore, the actual problem to solve can be written as

$$\begin{array}{ll} \text{minimize} & -\mathbf{c}_{sell}^{\intercal}\mathbf{p}_{sell} + \mathbf{c}_{buy}^{\intercal}\mathbf{p}_{buy} - \mathbf{c}_{a}^{\intercal}(\mathbf{p}_{b_l}^{-} + \mathbf{p}_{b_s}^{-}) \\ \text{subject to:} & \left[\mathbf{p}_{b}^{+}, \mathbf{p}_{b_l}^{-}, \mathbf{p}_{b_s}^{-}, \mathbf{p}_{g_l}, \mathbf{p}_{g_s}\right] \in \mathcal{X}_\omega \end{array}, \tag{2}$$

where $\omega \in \Omega$ is an uncertain parameter, and Ω is a set with cardinality equal to the number of the possible realizations of the constraints' set, which could also be infinite.

Given the impossibility of solving (2) for an infinite time horizon, Model Predictive Control (MPC) approaches have gained considerable attention in BESS control. The MPC method entails solving the optimization problem (2) within a predetermined time horizon. Subsequently, SoC is adjusted based on the obtained solution for a specific number of future time steps. Following these steps, estimations and initial values are updated, and the optimization problem (1) is solved again. This iterative process continuously optimizes control actions.

A. Literature review

In addressing uncertainties in (2) during MPC implementation, one may seek an optimizer that accommodates all potential realizations of constraints [10]. This strategy, commonly known as Robust MPC (RMPC), often yields highly conservative outcomes or even a null feasible space. To mitigate the conservativeness of RMPC, Carli *et al.* introduce a novel approach to tune the robustness property in multi-carrier microgrids with bounded uncertainties [11]. Nevertheless, this comes with the potential trade-off of compromising certain constraints in favor of reduced conservativeness. To enhance the feasibility of RMPC, Lan *et al.* introduce a non-anticipativity method that utilizes past available data to determine feasible control trajectories in [12]. However, it's worth noting that the resulting outcome may significantly differ from the optimal solution of (2). A two-stage RMPC procedure for multi-carrier microgrids is proposed in [13]. The first stage involves day-ahead scheduling, while the second stage employs a shrinking receding horizon approach to implement corrective actions. To mitigate the conservatiness of RMPC in multi-microgrids, Zhao *et al.* employ the distributed dynamic tube MPC [14]. While RMPC approaches show promise, there is a crucial concern regarding the recursive feasibility of the optimization problem (2) at all time steps.

Another strategy to adopt MPC in (2) is Stochastic MPC (SMPC). SMPC considers ω as a random variable with a probability $\mathbb{P}$ and finds a solution that may violate, at most, a fraction of constraints with a smaller probability of occurring than a predefined threshold. For instance, Parisio *et al.* introduce an SMPC strategy that involves a two-stage optimization process: initially, decisions about microgrid operations are made without considering the uncertainties; subsequently, once the uncertain variables' values are revealed, corrective actions are implemented [15]. In [16], SMPC is developed for multi-carrier multi-microgrid networks, and the generated scenarios are reduced using the mixed-integer linear programming method. In industrial applications, any risk associated with BESS's charging and discharging plan is unacceptable, as even a short interruption in production can result in significant losses outweighing the potential gains from optimizing the BESS unit's charge and discharge schedule. Consequently, SMPC is not favored in industries. Interested readers are referred to [17]–[19] for more details about the literature on optimal control of BESSs.

In industrial settings, where simplicity and robustness are paramount, rule-based control techniques for BESS [20], [21] often hold greater appeal than RMPC and SMPC. Rule-based approaches are favored for their ease of understanding, implementation, and inherent robustness against uncertainties. However, while rule-based controllers offer simplicity and robustness, MPC controllers generally provide more economically optimal results. In this paper, we propose a control strategy that aims to harness the advantages of both MPC and rule-based control techniques by integrating the strengths of MPC's optimization capabilities with the simplicity and robustness of rule-based control. In summary, the main advancements of our proposed rule-based MPC (RubPC) scheduling algorithm

Table I: Comparison with the State-of-the-art MPC-Based BESS Scheduling Approaches

	Seyednouri *et al.* [16]	Parisio *et al.* [15]	Zhao *et al.* [14]	Vasilj *et al.* [13]	Carli *et al.* [11]	RubPC
Prior knowledge about uncertainty space	Required	Required	Required	Required	Required	Not Required
Prior knowledge about uncertainties distribution	Required	Required	Not Required	Not Required	Not Required	Not Required
Scenario generation	Required	Required	Not Required	Required	Not Required	Not Required

compared to RMPC and SMPC are:

- **No prior knowledge requirement about uncertainties**: RMPC necessitates prior knowledge about the uncertainties' feasible space. This requirement becomes even more restrictive in SMPC, as it requires knowledge of the feasible space and the probability distribution of uncertainties. In contrast, RubPC does not require prior knowledge about uncertainties, making it more suitable for practical implementations.
- **Reduced optimization complexity**: Compared to RMPC and SMPC, RubPC offers lower computational complexity by eliminating the scenario generation phase in SMPC and reducing the number of constraints compared to RMPC. Given that these problems need to be solved repetitively, these methods often either demand expensive processors for control applications or experience delays in updating the optimal schedule of BESS, thereby reducing anticipated performance. In contrast, RubPC integrates a supervisory rule-based controller with a deterministic MPC. Given that the complexity of the rule-based controller, which involves conditional clauses, is relatively modest compared to MPC, which typically entails solving high-dimensional optimization problems, the overall complexity of RubPC does not significantly exceed that of deterministic MPC.

Table I compares several existing RMPC and SMPC methods designed for BESS scheduling in microgrids with uncertainties in load, and RES generated power with RubPC.

To our knowledge, [22] is the only published work combining rule-based control with MPC. In [22], the authors develop a two-stage framework. First, forecast scenarios of input conditions are generated. Then, to mitigate the complexity of the optimization problem, the number of scenarios is reduced. In the first stage, an SMPC is applied. Next, in the second stage, the actual on/off states of BESSs and thermostatically controlled loads are adjusted using a rule-based control method based on the results achieved by the SMPC. The main differences between the proposed algorithm in this article and the one presented in [22] are as follows:

- Pre-knowledge about the uncertainties is required in [22] since the optimal schedule is determined by using SMPC.
- The objective of integrating rule-based control with SMPC in [22] is to determine the states of BESSs, whereas, in the proposed method in this article, the objective of the rule-based controller is to maintain the microgrid states within a safe zone and ensure constraint satisfaction.

To summarize the literature review, several interesting approaches have been proposed to address the scheduling problem of BESSs in microgrids with uncertainties in load and RES-generated power. These approaches, mainly utilizing RMPC or SMPC, have shown promising results. However, they typically require degrees of prior knowledge about the uncertainties. Achieving recursive feasibility in classical RMPC methods and ensuring constraint satisfaction in SMPC remain open challenges for practically adopting these methods in the industry. This paper introduces a simple yet effective method to address these challenges.

B. Statement of Contributions

We propose RubPC, a rule-based MPC framework for scheduling the charge and discharge of BESSs in microgrids under power generation and load uncertainties. The proposed approach overcomes the main limitations of existing approaches by eliminating

1) the necessity for prior knowledge about load and RES generated power uncertainty bounds, as well as their probability distribution, in the BESS scheduling problem in microgrids;
2) the need for scenario generation to accommodate uncertainties in various situations.

We evaluated the proposed approach utilizing Monte Carlo analysis to verify constraint satisfaction through simulations conducted on a model constructed using data obtained from an actual construction site.

C. Organization

The remainder of this paper is organized as follows. Following this introduction, Section II presents the problem statements and introduces the associated constraints. Our proposed rule-based MPC Algorithm is presented in Section III. The simulation results are discussed in Section IV. Finally, Section V concludes this article.

D. Notation

A comprehensive nomenclature table is provided to explain the main notations used in this paper. Furthermore, we mean a coordinate-wise comparison when a comparison operator compares two vectors. In other words, let us denote the ith coordinate of $\mathbf{x}$ as $x(i)$, the notations $\mathbf{a} < \mathbf{b}$, $\mathbf{a} \leq \mathbf{b}$ and $\mathbf{a} = \mathbf{b}$ mean that $|\mathbf{a}| = |\mathbf{b}|$ and $a(i) < b(i)$, $a(i) \leq b(i)$ and

$a(i) = b(i)$ for all $i \in \{1, \dots, |\mathbf{a}|\}$, respectively. Finally, $\mathbf{a} \circ \mathbf{b}$ represents Hadamard product, i.e. if $|\mathbf{a}| = |\mathbf{b}|$ and $\mathbf{c} = \mathbf{a} \circ \mathbf{b}$, then $c(i) = a(i) \cdot b(i)$ for all $i \in \{1, \dots, |\mathbf{a}|\}$.

II. Problem Statement

The dynamics of BESS can be mathematically represented by [23]:

$$Q\frac{\partial \zeta}{\partial t} = \eta \mathbf{p}_b{}^+ + \mathbf{p}_{b_l^-} + \mathbf{p}_{b_s^-}, \tag{3}$$

where Q and ζ represent the capacity and SoC of BESS, respectively. Consistently to the notation introduced before, the charging power is denoted by $\mathbf{p}_b{}^+$. The power during a discharge, $\mathbf{p}_b{}^-$, is divided into two parts denoted as $\mathbf{p}_{b_l^-}$ and $\mathbf{p}_{b_s^-}$. $\mathbf{p}_{b_l^-}$ represents the power locally consumed during a discharge, and $\mathbf{p}_{b_s^-}$ is the power sold to the grid during a discharge. Throughout this paper, we quantify the charging power of BESSs by non-negative values, i.e., $\mathbf{p}_b{}^+ \geq 0$. In contrast, the discharging power is quantified by non-positive values, i.e., $\mathbf{p}_{b_l^-}, \mathbf{p}_{b_s^-} \leq 0$. Finally, $0 < \eta < 1$ represents the round trip efficiency.

Additionally, we assume the presence of a RES co-located with the BESS. The power generated by the RES can be further categorized into two parts, as outlined below:

$$\mathbf{p}_g = \mathbf{p}_{g_l} + \mathbf{p}_{g_s}, \tag{4}$$

where $\mathbf{p}_g$ stands for the total power generated by RES, $\mathbf{p}_{g_l}$ and $\mathbf{p}_{g_s}$ represent local consumption of the generated power (includes power consumption to charge the BESS) and power which is sold to the grid, respectively. We quantify $\mathbf{p}_g$, $\mathbf{p}_{g_l}$ and $\mathbf{p}_{g_s}$ with non-positive values in this article.

This paper proposes a novel rule-based MPC to establish a control strategy for the BESS. This approach is designed to handle uncertainties in load and RES power generation estimations effectively. Assume that T represents the length of the receding horizon time window. We denote the sampling time by Δt; thus, the total number of samples in the time window is equal to $q = \frac{T}{\Delta t}$. At each time step, our goal is to find a reference for the decision variables, $\mathbf{p}_b{}^+, \mathbf{p}_{b_l^-}, \mathbf{p}_{b_s^-}, \mathbf{p}_{gl}, \mathbf{p}_{g_s} \in \mathbb{R}^q$. BESS is subject to constraints, as discussed in the following subsection.

Remark 1. *While this article assumes the use of lithium-ion technology for BESS, which is currently the most common technology in power grids, it's important to note that RubPC can also be applied to microgrids employing various other BESS technologies or even alternative energy storage solutions such as pumped hydro storage [24], supercapacitors [25], thermostatically control loads [26], and flywheel energy storage [27]. Necessary adjustments to the constraints and degradation costs may be required for implementation.*

A. Constraints

Decision Variable Bounds

The decision variables $\mathbf{p}_b{}^+, \mathbf{p}_{b_l^-}, \mathbf{p}_{b_s^-}, \mathbf{p}_{g_l}$ and $\mathbf{p}_{g_s}$ are subject to the next bounds

$$\begin{array}{rcccl} \mathbf{0} & \leq & \mathbf{p}_b{}^+ & \leq & \mathbf{p}_b{}^{\max}, \\ \mathbf{p}_b{}^{\min} & \leq & \mathbf{p}_{b_l^-} & \leq & \mathbf{0}, \\ \mathbf{p}_b{}^{\min} & \leq & \mathbf{p}_{b_s^-} & \leq & \mathbf{0}, \\ \mathbf{p}_g & \leq & \mathbf{p}_{g_l} & \leq & \mathbf{0}, \\ \mathbf{p}_g & \leq & \mathbf{p}_{g_s} & \leq & \mathbf{0}, \end{array} \tag{5}$$

where $\mathbf{p}_g \in \mathbb{R}^q_-$ stands for estimated RES power generation. The maximum allowable charge and discharge power of each BESS is defined by $\mathbf{p}_b{}^{\max} \in \mathbb{R}^q_+$ and $\mathbf{p}_b{}^{\min} \in \mathbb{R}^q_-$, respectively. The following constraints are derived from the definition of decision variables

$$\begin{array}{rcl} \mathbf{p}_b{}^{\min} & \leq & \mathbf{p}_{b_l^-} + \mathbf{p}_{b_s^-}, \\ \mathbf{p}_g & = & \mathbf{p}_{g_l} + \mathbf{p}_{g_s}. \end{array} \tag{6}$$

Bound on the State of Charge (SoC)

The SoC of BESS must remain within the bounds stated by its manufacturing company.

$$\zeta^{\min} \leq \zeta \leq \zeta^{\max}, \tag{7}$$

where $\zeta^{\max} \in \mathbb{R}_+^{(q+1)}$ and $\zeta^{\min} \in \mathbb{R}_+^{(q+1)}$ represent the maximum and minimum allowable SoC, respectively. The dimensions of $\zeta^{\min}$, ζ and $\zeta^{\max}$ vectors in (7) have been chosen $q+1$ to be appropriate for (8), and the initial charge value has been added to ζ as its first index. It is worth noting that ζ is implicitly related to decision variables by

$$Q\mathbf{D}\zeta = \eta \mathbf{p}_b{}^+ + \mathbf{p}_{b_l^-} + \mathbf{p}_{b_s^-}, \tag{8}$$

where $\zeta \in \mathbb{R}_+^{(q+1)}$; and $\mathbf{D} \in \mathbb{R}^{q \times (q+1)}$ is defined as

$$\mathbf{D} = \frac{1}{\Delta t} \begin{bmatrix} -1 & 1 & 0 & . & . & 0 \\ 0 & -1 & 1 & 0 & . & 0 \\ & & . & . & & \\ & & & . & & \\ 0 & & & 0 & -1 & 1 \end{bmatrix}_{q \times (q+1)},$$

to approximate the derivative operator in (3).

Kinetic battery model

The relation between SoC and the power limits is usually represented by the kinetic battery model [28]. The feasible region for AC power described by the kinetic battery model is depicted in Fig. 1, which is the intersection of charge, discharge, and SoC bounds with a region delimited by two lines,

$$m^1\zeta + b^1 \leq \mathbf{p}_b{}^+ + \mathbf{p}_{b_l^-} + \mathbf{p}_{b_s^-} \leq m^2\zeta + b^2, \tag{9}$$

where m^1 and b^1 are the slope and intercept of the power limit on discharge, respectively, and m^2 and b^2 are the slope and intercept of the power limit on charge, respectively.

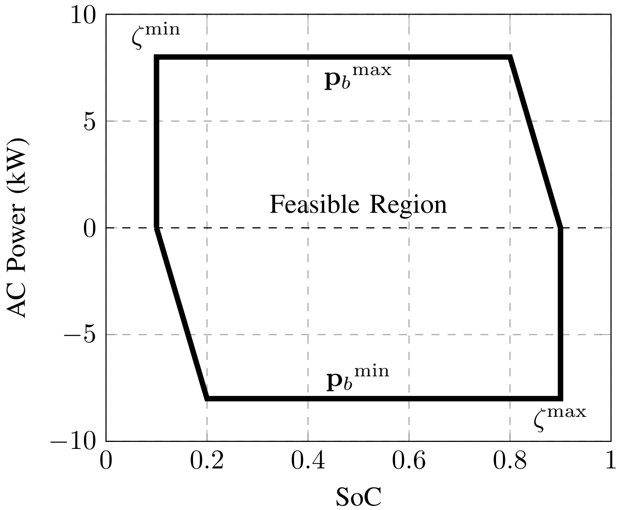

Fig. 1: Feasible region for AC power described by the kinetic battery model.

Constraints on power flow

In industrial loads, the power flow between customers and the grid is limited due to the installed infrastructure or the contract. This constraint is expressed as:

$$\mathbf{p}_b{}^{+} + \mathbf{p}_{b_l}{}^{-} + \mathbf{p}_l + \mathbf{p}_{g_l} \leq \mathbf{p}_l{}^{\max}, \tag{10}$$

$$-\mathbf{p}_{b_s}{}^{-} - \mathbf{p}_{g_s} \leq \mathbf{p}_l{}^{\max}. \tag{11}$$

where $\mathbf{p}_l \in \mathbb{R}_+^q$ represent the local power consumption, excluding the power consumption of BESS, and $\mathbf{p}_l{}^{\max} \in \mathbb{R}_+^q$ is the upper bound of the industrial microgrid power exchange with the utility grid.

Remark 2. *Our proposed method applies to both grid-connected and islanded microgrids. The microgrid operates in islanded mode if the maximum power flow with the grid is set to zero, i.e.,* $\mathbf{p}_l{}^{\max} = 0$ *in* (10) *and* (11). ■

Local power balance constraint

We denoted with separate variables the power used to charge the BESS, $\mathbf{p}_b{}^{+}$, the power consumed by the local load, $\mathbf{p}_l$, the power output of the BESS during a discharge, $\mathbf{p}_{b_l}{}^{-}$, which is consumed locally, the local power generation consumed locally, $\mathbf{p}_{g_l}$. Since the sum of the local power generation and the output power of the BESS consumed locally cannot exceed the actual local load consumption, it follows that:

$$\mathbf{p}_b{}^{+} + \mathbf{p}_l + \mathbf{p}_{b_l}{}^{-} + \mathbf{p}_{g_l} \geq \mathbf{0}. \tag{12}$$

B. Objective Function

$\mathbf{p}_{buy}$ and $\mathbf{p}_{sell}$ in our problem are

$$\begin{array}{rcl} \mathbf{p}_{buy} & = & \mathbf{p}_b{}^{+} + \mathbf{p}_{b_l}{}^{-} + \mathbf{p}_l + \mathbf{p}_{g_l}, \\ \mathbf{p}_{sell} & = & -\mathbf{p}_{b_s}{}^{-} - \mathbf{p}_{g_s}. \end{array} \tag{13}$$

The lifetime of a battery depends on various factors, including the type of battery, depth of discharge, charging and discharging rates, temperature conditions, and overall battery management [29]–[31]. As a result, accurately estimating a battery's lifetime is a complex task. However, a reasonable estimate can be derived based on the number of charge cycles a battery typically undergoes. Therefore, the degradation cost could be represented by

$$c_a = \frac{\text{Battery Price}}{\text{Capacity} \times \text{Lifetime charge cycles}}. \tag{14}$$

For the sake of smoothing the optimization formulas, we assume that the degradation cost is constant, i.e., all coordinates of $\mathbf{c}_a \in \mathbb{R}_+^q$ are c_a. However, the degradation cost in (15) can be replaced with any other model or representation without affecting the generality of our approach. Additionally, we assume that battery replacement and maintenance costs are incorporated into the degradation cost. Otherwise, they should be added as penalties to the objective function in (15).

Noticing that we are interested in control strategies that do not interfere with the production plan of the factory, we assume that control of $\mathbf{p}_l$ is not allowed. Therefore, $\mathbf{c}_{sell}^{\intercal}\mathbf{p}_l$ becomes a constant that can be removed from the objective function in (2). Consequently, considering (13), (2) can be rewritten as:

$$\begin{array}{rl} \text{minimize} & \mathbf{c}_{sell}^{\intercal}(\mathbf{p}_{b_s}{}^{-} + \mathbf{p}_{g_s}) + \mathbf{c}_{buy}^{\intercal}(\mathbf{p}_b{}^{+} + \mathbf{p}_{b_l}{}^{-} + \mathbf{p}_{g_l}) \\ & - \mathbf{c}_a^{\intercal}(\mathbf{p}_{b_l}{}^{-} + \mathbf{p}_{b_s}{}^{-}) \\ \text{subject to:} & \left[\mathbf{p}_b{}^{+}, \mathbf{p}_{b_l}{}^{-}, \mathbf{p}_{b_s}{}^{-}, \mathbf{p}_{g_l}, \mathbf{p}_{g_s}\right] \in \mathcal{X}_\omega. \end{array} \tag{15}$$

It is worth reminding that since $\mathbf{p}_g$ and $\mathbf{p}_l$ are subject to uncertainties, the feasible space of decision variables is not deterministic. Therefore, we used $\mathcal{X}_\omega$ in (15) to define the feasible space of decision variables according to (5)-(12) and to account for this uncertainty. In this paper, we assume the following assumptions hold for the microgrid and tariffs.

Assumption 1. *The discrepancies between actual and predicted load and RES generated power in the microgrid are bounded.* ■

Assumption 1 is necessary to satisfy (10) and (11), and it is quite trivial because neither the actual load and RES-generated power nor their estimated values could reasonably be infinite.

Furthermore, In the microgrid setting that we discuss in this study, comprising load, RES, and BESS, where power flow is restricted, any shortfall in energy required by the load beyond what local generation can provide must either be supplemented by the utility or drawn from the BESS. Exceeding the maximum allowed power flow is unsustainable, as continued reliance on the BESS will eventually lead to complete discharge. Thus, in addition to Assumption 1, it is necessary for the following assumption to hold true.

Assumption 2. *There is a feasible dispatch plan within the microgrid for any finite time intervals, T_i, that satisfies all constraints.* ■

It is important to emphasize that Assumption 1 and Assumption 2 establish only the necessary conditions for finding a feasible plan. Therefore, it is sensible to incorporate greater flexibility into the microgrid design. Greater flexibility in the microgrid dispatch can be achieved by increasing the BESS capacity and/or the maximum allowable power flow with the

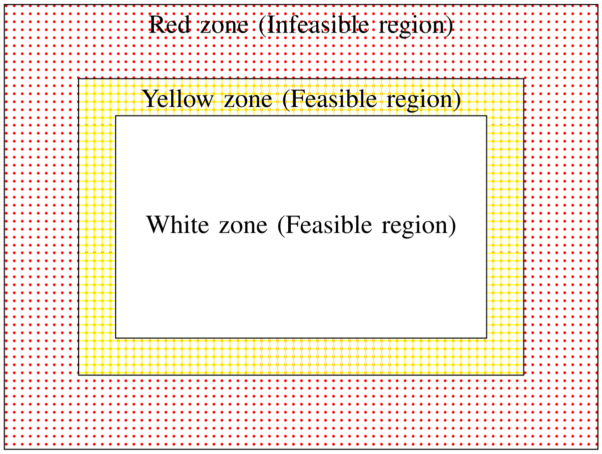

Fig. 2: Red, yellow, and white zones.

utility grid.

Furthermore, our approach assumes the following regarding tariffs.

Assumption 3. *This paper assumes that the utility considers an overhead for its services, i.e.,* $\mathbf{c}_{buy} - \mathbf{c}_{sell} > \mathbf{0}$. ■

Remark 3. *Assumption 3 ensures that the optimal solution of* (15) *does not involve simultaneous selling and purchasing of energy. Furthermore, in* (8), $\eta < 1$ *prevents simultaneous BESS charging and discharging in the optimal plan. Therefore, it is possible to neglect nonlinear constraints such as* $\mathbf{p}_{buy} \circ \mathbf{p}_{sell} = \mathbf{0}$ *and* ${\mathbf{p}_b}^+ \circ ({\mathbf{p}_{b_s}}^- + {\mathbf{p}_{b_l}}^-) = \mathbf{0}$. ■

III. Rule-Based Predictive Control of BESS (RubPC)

The main idea of our proposed method is based on dividing the feasible region of decision variables into two sub-zones: the "white" and "yellow" zones, and the entire infeasible region is referred to as the "red" zone, i.e., for simplicity, depicted in two dimensions in Fig. 2. The yellow zone serves as the boundary space between the white and red zones and determines the "feasible" operation of BESS, but close to violating certain constraints. The width of the yellow zone depends on specific load characteristics, fluctuations in the RES-generated power, and the parameters of the BESS. However, It should ensure sufficient control room to prevent uncertainties from disrupting the system.

Drawing inspiration from supervisory control methods in BESS, such as [32], we design a two-level controller system. In the first level, we implement an MPC to maintain the system's operation within the white zone. Additionally, a rule-based control is proposed for the second level. This rule-based controller is designed to take corrective actions when the system falls into the yellow zone due to estimation errors. It is important to note that the rule-based control does not focus on optimization but instead aims to select the most effective control action to bring the micro-grid parameters back to the white zone.

A. White Zone Boundary

We assume the following safety margins regarding the allowable SoC bound and the power exchange limit with the grid:

$$\zeta^{\min} + \alpha \le \zeta \le \zeta^{\max} - \alpha, \tag{16}$$

$$\mathbf{p}_b{}^+ + {\mathbf{p}_{b_l}}^- + \mathbf{p}_l + \mathbf{p}_{g_l} \le \mathbf{p}_l{}^{\max} - \beta, \tag{17}$$

$$-{\mathbf{p}_{b_s}}^- - \mathbf{p}_{g_s} \le \mathbf{p}_l{}^{\max} - \beta, \tag{18}$$

where $\alpha \in \mathbb{R}_+^{(q+1)}$ and $\beta \in \mathbb{R}_+^q$ represent safety margins for the SoC and the power exchange limit with the grid, respectively. Thus, (16), (17) and (18) must replace (7),(10) and (11) to find a solution that lies in the white zone.

B. Supervisory Rules

The rule-based controller should track and keep the SoC and power exchange values within the white zone. It is important to note that, under ideal conditions without uncertainties, the microgrid's power exchange with the utility grid and the SoC of the BESS remain within the white zone, requiring no intervention. However, if forecast errors occur, these parameters may deviate from the white zone. The microgrid has exited the white zone if one or more of the following conditions are met:

- $\zeta(t_k) < (\zeta^{\min} + \alpha)$. This means that the BESS SoC is approaching its lower bound, so the most sensible action for the safe operation of a microgrid is to charge the BESS to bring it back within the white zone.
- $\zeta(t_k) > (\zeta^{\max} - \alpha)$. In contrast to the previous situation, this case indicates that the BESS SoC is now close to its upper bound. To maintain capacity for future maneuvers and ensure the safe dispatch of the microgrid in the presence of uncertainties, it is necessary to discharge the BESS and bring the SoC back within the white zone.
- $p_{buy}(t_k) > {p_l}^{\max}(t_k) - \beta$. This situation indicates that the power flow from the utility grid to the microgrid has exceeded the safety bound. Therefore, the reasonable decision is to use the energy stored in the BESS by discharging it to ensure the safe and secure operation of the microgrid.
- $p_{sell}(t_k) > {p_l}^{\max}(t_k) - \beta$. Similar to the previous situation, there could be a case where the RES-generated power in the microgrid exceeds local needs and should be transferred to the utility grid. Suppose the transferred power exceeds the safety margins. In that case, the available capacity of the BESS should be used to absorb a portion of this power to ensure the safe operation of the microgrid.

Therefore, sensible charging and discharging actions should be taken on the BESS unit to address scenarios when the microgrid enters the yellow zone. To determine a feasible charging power of the BESS, we should verify that

- The charging (discharging) power is lower (higher) than the maximum allowable charging (discharging) power, ${p_b}^{\max}$ (${p_b}^{\min}$), ensuring that that (5) is satisfied.

- The charging (discharging) power satisfies the kinetic battery model (9), meaning it should be lower (higher) than $m^2\zeta(t_k)+b^2$ ($m^1\zeta(t_k)+b^1$).
- Neglecting the BESS, the term $-p_l(t_k)-p_g(t_k)$ represents the power that needs to be transferred to the utility grid at time step t_k based on the RES generated power and load. Considering that we quantify generated power with non-positive values in this paper, $-p_l(t_k)-p_g(t_k)>0$ implies that the generated power exceeds the local power needs, and similarly, $-p_l(t_k)-p_g(t_k)<0$ means that local power consumption is greater than power generation. Recall that ${p_l}^{\max}(t_k)$ represents the maximum power transfer capacity at time step t_k, since it is already occupied by $-p_l(t_k)-p_g(t_k)$, the remaining capacity, considering the safety margin introduced in (17) and (18), is ${p_l}^{\max}(t_k)-p_l(t_k)-p_g(t_k)-\beta$ for charging and ${p_l}^{\max}-p_l(t_k)-p_g(t_k)+\beta$ for discharging.

The following conditional rules mathematically represent the logic discussed regarding the necessary actions the BESS should take when the microgrid enters the yellow zone.

$$\text{If}\quad \zeta(t_k)<(\zeta^{\min}+\alpha)\quad\text{then:}$$
$$\begin{cases} {p_b}^{+}(t_k)=\min\{m^2\zeta(t_k)+b^2,{p_b}^{\max}(t_k),\\ \qquad\qquad {p_l}^{\max}(t_k)-p_l(t_k)-p_g(t_k)-\beta\},\\ {p_b}^{-}(t_k)=0. \end{cases} \tag{19a}$$

$$\text{If}\quad \zeta(t_k)>(\zeta^{\max}-\alpha)\quad\text{then:}$$
$$\begin{cases} {p_b}^{+}(t_k)=0,\\ {p_b}^{-}(t_k)=\max\{m^1\zeta(t_k)+b^1,{p_b}^{\min}(t_k),\\ \qquad\qquad -{p_l}^{\max}-p_l(t_k)-p_g(t_k)+\beta\}. \end{cases} \tag{19b}$$

$$\text{If}\quad p_{buy}(t_k)>{p_l}^{\max}(t_k)-\beta\quad\text{then:}$$
$$\begin{cases} {p_b}^{+}(t_k)=0,\\ {p_b}^{-}(t_k)=\max\{m^1\zeta(t_k)+b^1,{p_b}^{\min}(t_k),\\ \qquad\qquad -{p_l}^{\max}-p_l(t_k)-p_g(t_k)+\beta\}. \end{cases} \tag{19c}$$

$$\text{If}\quad p_{sell}(t_k)>{p_l}^{\max}(t_k)-\beta\quad\text{then:}$$
$$\begin{cases} {p_b}^{+}(t_k)=\min\{m^2\zeta(t_k)+b^2,{p_b}^{\max}(t_k),\\ \qquad\qquad {p_l}^{\max}(t_k)-p_l(t_k)-p_g(t_k)-\beta\},\\ {p_b}^{-}(t_k)=0. \end{cases} \tag{19d}$$

In (19a), we address the situation where the SoC is so close to its lower bound that it has entered the yellow zone, so the sensible action is to charge the BESS. However, the charging power must satisfy the kinetic model of BESS, ${p_b}^{+}(t_k)\le m^2\zeta(t_k)+b^2$ and the charging upper bound, ${p_b}^{+}(t_k)\le {p_b}^{\max}(t_k)$. On the other hand, the charging power should not exceed the power transfer capacity. Considering that ${p_l}^{\max}(t_k)$ represents the maximum power transfer capacity at time step t_k, and it is already occupied by $-p_l(t_k)-p_g(t_k)$, the remaining capacity, considering the safety margin introduced in (18), is ${p_l}^{\max}(t_k)-p_l(t_k)-p_g(t_k)-\beta$. This results in $p_b^{+}(t_k)\le {p_l}^{\max}(t_k)-p_l(t_k)-p_g(t_k)-\beta$. Consequently, the best charging power for BESS to exit the yellow zone and return to the white zone is ${p_b}^{+}(t_k)=\min\{m^2\zeta(t_k)+b^2,{p_b}^{\max}(t_k),{p_l}^{\max}(t_k)-p_l(t_k)-p_g(t_k)-\beta\}$. Similar reasoning applies to (19b), (19c), and (19d).

Let's delve deeper into the rules introduced in (19a)-(19d). For instance, if $p_{buy}(t_k)>{p_l}^{\max}(t_k)-\beta$, according to (19c), BESS starts discharging at a sufficiently high power to compensate for the excess power exchange. Notably, in this rule, we have not included the safety boundary margins of SoC, represented by α. Consequently, the BESS can discharge to $\zeta^{\min}$. In other words, we prioritize power exchange with the grid. If both SoC and power exchange enter the yellow zone, we will first implement appropriate charge and discharge actions to keep the power exchange within the white zone, even if this decision keeps the SoC in the yellow zone. However, designers can easily modify the priority order of constraints to align with the specific requirements in their industrial context.

It is important to note that if the SoC falls into the yellow zone, and there is no available capacity for compensation, both charge and discharge powers will be set to zero according to (19a) and (19b). However, given that the lack of available capacity indicates a violation of one of the power exchange boundaries, according to our proposed ordering, the charge and discharge powers will be overwritten based on (19c) or (19d).

Remark 4. *Without uncertainties, MPC ensures that BESS operates optimally within the predefined white zone without intervention from the rule-based controller. However, in scenarios where forecast errors occur, the rule-based controller adjusts the MPC-generated schedule to maintain system stability by keeping states within the white zone. This adjustment increases with the increase in forecast errors, leading to greater reliance on the rule-based schedule for safety assurance. Since the rule-based controller prioritizes system safety, it may not produce an optimally efficient schedule. Consequently, as forecast errors escalate, the resulting schedule deviates further from the optimal solution as the system prioritizes stability and constraints by following the rule-based controller plans instead of the MPC-generated ones.*

C. Algorithm

Algorithm 1 represents our proposed Rule-Based Predictive Control of BESS (RubPC). In Phase 1 of RubPC, $\mathbf{p}_l$ and $\mathbf{p}_g$ are estimated for the upcoming q time samples. In Phase 2, we solve the optimization problem introduced in Section II within the T-width time horizon, based on the estimations of $\mathbf{p}_l$ and $\mathbf{p}_g$. Consequently, we determine the reference signals of ${\mathbf{p}_b}^{+}$ and ${\mathbf{p}_b}^{-}$ for the next T_c time steps, where ${\mathbf{p}_b}^{-}={\mathbf{p}_b}_l^{-}+{\mathbf{p}_b}_s^{-}$. In Phase 3, at each time step, $t_k=1,\dots,T_c$, where $t_k=1$ is the first time step in the control horizon, RubPC evaluates whether the current charge or discharge reference of BESS keeps the states within the white zone. This evaluation considers the actual load and RES-generated power values, which may differ from the estimated values when the MPC was executed.

Algorithm 1 Rule-Based Predictive Control of BESS (RubPC)

Require: Δt, T, T_c, ${\mathbf{p}_b}^{\min}$, ${\mathbf{p}_b}^{\max}$, ${\mathbf{p}_l}^{\max}$, $\zeta^{\min}$, $\zeta^{\max}$, m^1, b^1, m^2, b^2, β, α, Q, η.
Start
Phase 1: Estimation and Update
Estimate $\mathbf{p}_l$ and $\mathbf{p}_g$ for the upcoming q time samples.
Update $\mathbf{c}_{buy}$ and $\mathbf{c}_{sell}$ for the upcoming q time samples.
Phase 2: Optimization
Solve (15) and find the optimal ${\mathbf{p}_b}^+$ and ${\mathbf{p}_b}^-$ (In white zone).
Phase 3: Control
for $t_k = 1, \ldots, T_c$ **do**
Check (19a)-(19d), and if needed, update ${p_b}^+(t_k)$ and ${p_b}^-(t_k)$.
Apply ${p_b}^+(t_k)$ and ${p_b}^-(t_k)$ to the BESS.
end for
Go to Phase 1.
End

Table II: RubPC and BESS parameters in numerical simulation

Par.	Value	Par.	Value	Par.	Value
Δt	$60s$	Q	$1500kWh$	$\zeta^{\min}$	0.1
T	$24h$	${\mathbf{P}_b}^{\max}$	$150kW$	$\zeta^{\max}$	0.9
T_c	$0.25h$	${\mathbf{P}_b}^{\min}$	$300kW$	m^1	-3000
${\mathbf{P}_l}^{\max}$	$700kW$	η	0.96	m^2	-1500
β	$20kW$	b^1	$-\zeta^{\min}m^1$		
α	0.05	b^2	$-\zeta^{\max}m^2$		

IV. Numerical Simulation

To evaluate the performance of RubPC, as depicted in Fig. 3, we consider a simulation testbed designed based on data of power consumption and RES-generated power in an electrified quarry site located near Gothenburg, Sweden, equipped with solar panels and a BESS. The RubPC and BESS parameters are presented in Table II. The quarry location yields gravel, aggregate, and sand at a daily production rate of 6,000 tons. The construction machinery used at this quarry includes wheel loaders, excavators, and dump trucks.

A simulation framework was developed in [33] tailored for modeling off-road transport operations in construction worksites, focusing on using electric construction equipment. In this framework, a dynamic model was developed to depict the electric dump trucks' longitudinal behavior accurately. The model's outputs are subsequently integrated into a fleet model, enabling the performance evaluation of transport efficiency. Within the fleet model, a discrete-event simulation technique is employed to effectively represent the transport operations' logistics. This technique facilitates capturing interactions among the vehicles and resources, providing a comprehensive understanding of the operational dynamics.

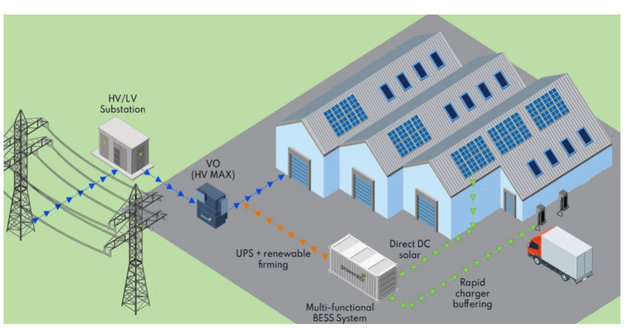

Fig. 3: Simplified architecture of worksite microgrid.

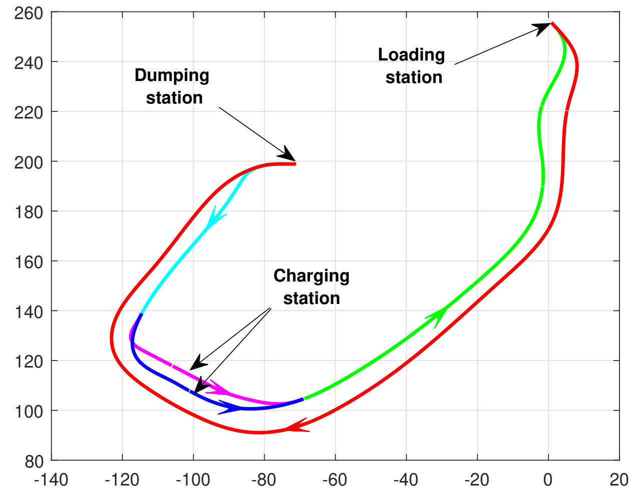

Fig. 4: Site layout. The transport paths are illustrated using different colors.

A. Experimental Setup

An experiment was conducted using the autonomous battery-electric dump trucks, referred to as “HXs” hereafter, in the quarry's transportation operation for a period exceeding 10 weeks. A specific geographical area was designated for this experiment, where any interaction with manually operated vehicles and humans was strictly prohibited within the dedicated operational zone. In this experimental setup, 8 identical HXs were available.

Fig. 4 shows the layout of the transport operation, including service stations for loading, dumping, and charging. These service stations operate on a first-come, first-served basis, each with a maximum service capacity. The loading station (LS) and dumping station (DS) have a service capacity limit of one HX at a time. In contrast, the charging station (CS) offers two parallel charging spots, and an HX will use the first available charging spot upon arrival. Queue systems are implemented before each service station. If another HX occupies a service station, the waiting HXs line up in their respective queues. In this experiment, HXs are charged up to their full capacity before leaving the charging station, so the service time, or charging time, depends on the SoC level of the vehicle upon arrival.

The operation consists of the following processes:

1) Loading (the wheel loader loads material into the HXs)
2) Transport (the HXs transport material from the loading station to the dumping station, and the transport path is marked in red in Fig. 3)
3) Dumping (the HXs deposit material into the crusher at the dumping station)

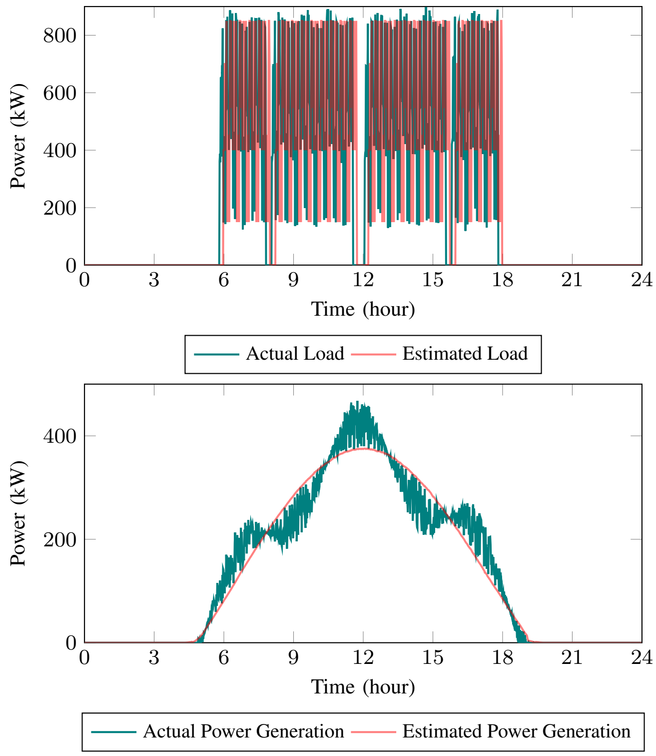

Fig. 5: Actual and estimated load and generated power in our simulation case study.

4) Transport (the HXs travel to the charging station, and the path is marked in cyan in Fig. 4)
5) Charging (the battery of HXs is charged to a required level)
6) Transport (the HXs return to the loading station, and the path is given in green in Fig. 4)

In our case study, the primary sources of energy consumption are the CSs, where HXs charge their batteries and grid-connected machinery, such as rock crushers. Estimating the load of this electrified quarry site is challenging because even a small variation in the working schedule and the load of the machinery can significantly shift the overall load. Additionally, the power generated by solar panels could differ from the estimated values. The actual and estimated generated power and load in a sample day are depicted in Fig. 5.

The purchasing electricity price in a sample day, $\mathbf{c}_{buy}$, is depicted in Fig. 6. We assume $\mathbf{c}_{sell} = 0.9 \cdot \mathbf{c}_{buy}$. Furthermore, we consider the lifetime cycles of the BESS to be 2000 [34] and the cost of the BESS is 1000 SEK (Swedish Krona) per kW, thus from (14), $\mathbf{c}_a = 0.5$SEK.

B. Simulations

To validate RubPC's effectiveness, we corroborate it from two perspectives. First, we consider only a sample day and compare the results achieved by RubPC with conventional MPC, a rule-based strategy that does not use prediction for control, and the case without BESS installation. Next, we verify RubPC's capability to satisfy the microgrid constraints by performing Monte Carlo simulations.

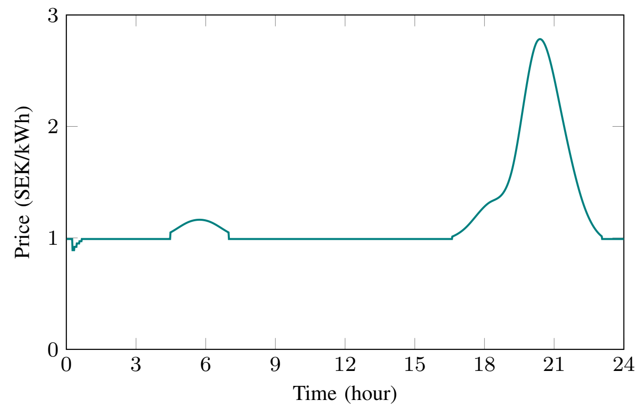

Fig. 6: The purchasing electricity price, $\mathbf{c}_{buy}$, in a sample day.

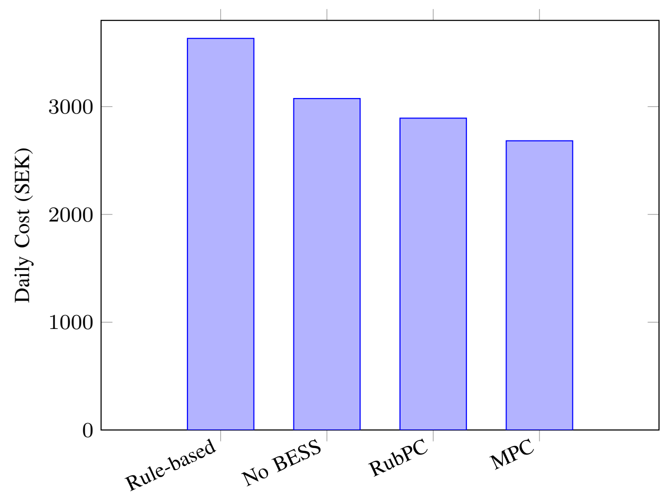

Fig. 7: Comparison of the daily electrical energy cost in our case study without BESS and with BESS controlled using RubPC, MPC, and Rule-based control. Note that the BESS degradation cost is included in RubPC and MPC Rule-based control costs.

1) Simulation in a Sample Day: Fig. 7 compares the daily electrical energy prices under different scenarios: the implementation of RubPC, conventional MPC, no BESS installation, and a rule-based strategy designed to maintain $SoC = 0.5$. In this strategy, the BESS is charged and discharged as needed to satisfy (10) and (11). It is essential to note that the BESS degradation cost is included in the overall costs when the BESS is discharged.

As observed, implementing RubPC leads to a slight increase in daily costs compared to MPC. This is attributed to the microgrid occasionally entering the yellow zone due to load and RES-generated power estimations inaccuracies. During such instances, we transition from optimal control to rule-based control, prioritizing the return of states to the white zone rather than achieving optimality. Consequently, we should not anticipate better cost-wise outcomes than MPC since we compromise optimality for reliable control actions, ensuring that microgrid and BESS constraints are not violated.

In Fig. 8, it becomes apparent that conventional MPC faces

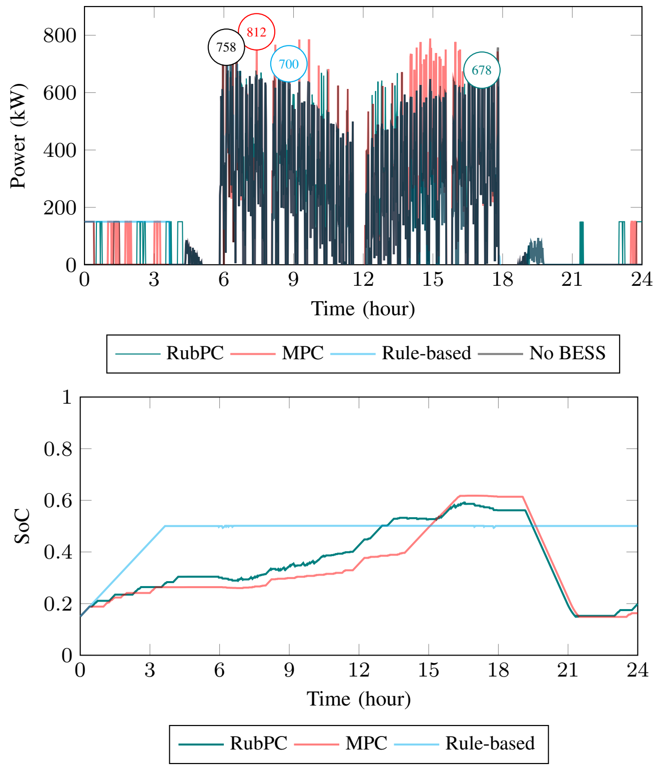

Fig. 8: Power flow with the grid (top) and the SoC of the BESS unit (bottom) in different scenarios. The maximum values of power flow in different scenarios are written in circles.

challenges in ensuring constraint satisfaction. The power flow, expected to remain below 700, surpasses this limit, reaching up to 812. This constraint violation poses a significant risk to the secure operation of infrastructures and may lead to substantial penalty costs that the factory could incur for exceeding the maximum power demand allowance. In contrast, RubPC and Rule-based control strategies effectively satisfy power flow constraints.

The collective insights from Figs. 7 and 8 underscore that RubPC adeptly integrates the optimal characteristics of MPC to yield cost-effective controls. Simultaneously, it incorporates the robust features inherent in Rule-based controls. This dual capability positions RubPC as a compelling approach, proficiently balancing cost considerations with robustness in constraint satisfaction.

2) Monte Carlo Verification of Constraints Satisfaction: To assess RubPC in meeting constraints amidst varying stochastic discrepancies in actual-predicted load and RES power generation, we conducted 1000 Monte Carlo simulations. These simulations incorporate average forecast errors of 7% for RES generation power [35] and 100% for load, considering that the average load could replace the estimation in challenging estimation cases. The top plots in Fig. 9 illustrate the distribution of maximum and minimum power flow to the grid, while the bottom plots display the distribution of maximum and minimum SoC of the BESS. As depicted in Fig. 9, the implementation of RubPC successfully fulfills constraints amid diverse discrepancy variations in actual-predicted load and RES power generation.

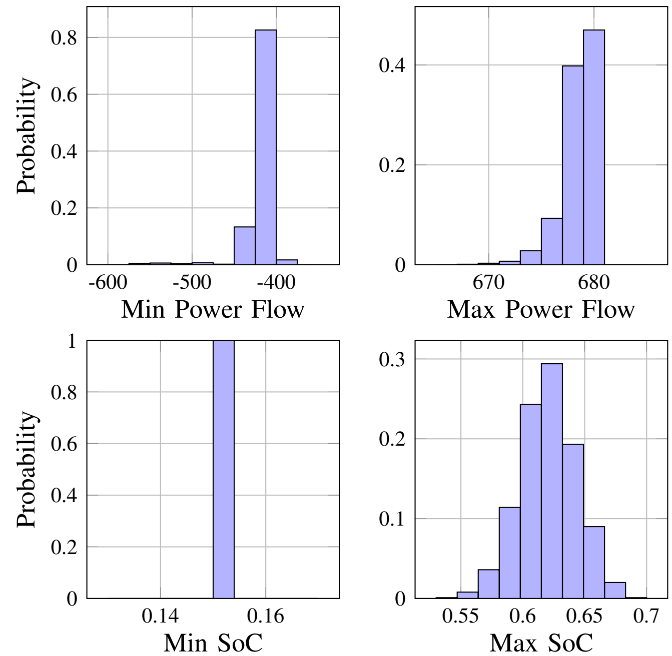

Fig. 9: Probability distribution functions for the minimum and maximum grid power flow (top) and the minimum and maximum SoC of BESS unit (bottom) in 1000 Monte Carlo simulations.

V. Conclusion

The RubPC introduced in this paper is a straightforward yet effective algorithm for controlling the SoC in industrial BESS units, especially when load and local power generation cannot be precisely estimated. Initially, we partition the feasible space of decision variables into two sub-zones: the "white" and "yellow" zones, with the yellow zone serving as the boundary space between the white and infeasible zones. The key concept involves incorporating a safety buffer, the yellow zone, when applying MPC to control the BESS. This buffer ensures sufficient control room for rule-based control to address discrepancies between actual and estimated values, which could jeopardize the satisfaction of microgrid and BESS constraints. To implement this, we use MPC to keep the states within the white zone, while the rule-based control acts as a supervisory controller. If the states enter the yellow zone, the rule-based control adjusts the control action to bring the states back to the white zone. Our numerical simulation on an electrified quarry site, characterized by significant load fluctuations and inaccurate load and local power generation estimates, demonstrates that RubPC adeptly manages uncertainties in estimations and fulfills microgrid and BESS constraints. In future studies, it would be valuable to explore the application of RubPC in complex microgrids with multiple BESSs. The goal is to synchronize these systems collaboratively and minimize costs while meeting constraints in the context of inaccurate load and RES generation forecasts.

References

[1] M. A. Khan, A. Haque, and V. S. B. Kurukuru, "Power flow management with Q-learning for a grid integrated photovoltaic and energy storage system," *IEEE Journal of Emerging and Selected Topics in Power Electronics*, vol. 10, no. 5, pp. 5762–5772, 2022.

[2] A. Bartolini, F. Carducci, C. B. Muñoz, and G. Comodi, "Energy storage and multi energy systems in local energy communities with high renewable energy penetration," *Renewable Energy*, vol. 159, pp. 595–609, 2020.

[3] H. Su, D. Feng, Y. Zhao, Y. Zhou, Q. Zhou, C. Fang, and U. Rahman, "Optimization of customer-side battery storage for multiple service provision: Arbitrage, peak shaving, and regulation," *IEEE Transactions on Industry Applications*, vol. 58, no. 2, pp. 2559–2573, 2022.

[4] N. Mignoni, P. Scarabaggio, R. Carli, and M. Dotoli, "Control frameworks for transactive energy storage services in energy communities," *Control Engineering Practice*, vol. 130, p. 105364, 2023.

[5] M. Kaheni, A. Pilloni, G. S. Ruda, E. Usai, and M. Franceschelli, "Distributed asynchronous greedy control of large networks of thermostatically controlled loads for electric demand response," *IEEE Control Systems Letters*, vol. 7, pp. 169–174, 2023.

[6] Q. Huang, L. Yang, Q.-S. Jia, Y. Qi, C. Zhou, and X. Guan, "A simulation-based primal-dual approach for constrained V2G scheduling in a microgrid of building," *IEEE Transactions on Automation Science and Engineering*, vol. 20, no. 3, pp. 1851–1863, 2023.

[7] M. Kaheni, E. Usai, and M. Franceschelli, "A distributed optimization and control framework for a network of constraint coupled residential BESSs," in *2021 IEEE 17th International Conference on Automation Science and Engineering (CASE)*. IEEE, 2021, pp. 2202–2207.

[8] X. Chen, Y. Yang, J. Song, J. Wang, and G. He, "Hybrid energy storage system optimization with battery charging and swapping coordination," *IEEE Transactions on Automation Science and Engineering*, vol. 21, no. 3, pp. 4094–4105, 2024.

[9] A. Gailani, M. Al-Greer, M. Short, and T. Crosbie, "Degradation cost analysis of Li-Ion batteries in the capacity market with different degradation models," *Electronics*, vol. 9, no. 1, p. 90, 2020.

[10] D. Q. Mayne, "Model predictive control: Recent developments and future promise," *Automatica*, vol. 50, no. 12, pp. 2967–2986, 2014.

[11] R. Carli, G. Cavone, T. Pippia, B. De Schutter, and M. Dotoli, "Robust optimal control for demand side management of multi-carrier microgrids," *IEEE Transactions on Automation Science and Engineering*, vol. 19, no. 3, pp. 1338–1351, 2022.

[12] Y. Lan, Q. Zhai, C.-B. Yan, X. Liu, and X. Guan, "Robust approximate dynamic programming for large-scale unit commitment with energy storages," *IEEE Transactions on Automation Science and Engineering*, vol. 21, no. 4, pp. 7401–7412, 2024.

[13] J. Vasilj, D. Jakus, and P. Sarajcev, "Robust nonlinear economic MPC based management of a multi energy microgrid," *IEEE Transactions on Energy Conversion*, vol. 36, no. 2, pp. 1528–1536, 2021.

[14] Z. Zhao, J. Xu, J. Guo, Q. Ni, B. Chen, and L. L. Lai, "Robust energy management for multi-microgrids based on distributed dynamic tube model predictive control," *IEEE Transactions on Smart Grid*, vol. 15, no. 1, pp. 203–217, 2024.

[15] A. Parisio, E. Rikos, and L. Glielmo, "Stochastic model predictive control for economic/environmental operation management of microgrids: An experimental case study," *Journal of Process Control*, vol. 43, pp. 24–37, 2016.

[16] S. Seyednouri, A. Safari, M. Farrokhifar, S. N. Ravadanegh, A. Quteishat, and M. Younis, "Optimal stochastic scheduling of a multi-carrier multi-microgrid system considering storages, demand responses, and thermal comfort," *Sustainable Cities and Society*, vol. 99, p. 104943, 2023.

[17] Y. Yang, S. Bremner, C. Menictas, and M. Kay, "Modelling and optimal energy management for battery energy storage systems in renewable energy systems: A review," *Renewable and Sustainable Energy Reviews*, vol. 167, p. 112671, 2022.

[18] B. Chreim, M. Esseghir, and L. Merghem-Boulahia, "Recent sizing, placement, and management techniques for individual and shared battery energy storage systems in residential areas: A review," *Energy Reports*, vol. 11, pp. 250–260, 2024.

[19] M. Hossain Lipu, S. Ansari, M. S. Miah, K. Hasan, S. T. Meraj, M. Faisal, T. Jamal, S. H. Ali, A. Hussain, K. M. Muttaqi, and M. Hannan, "A review of controllers and optimizations based scheduling operation for battery energy storage system towards decarbonization in microgrid: Challenges and future directions," *Journal of Cleaner Production*, vol. 360, p. 132188, 2022.

[20] S. Teleke, M. E. Baran, S. Bhattacharya, and A. Q. Huang, "Rule-based control of battery energy storage for dispatching intermittent renewable sources," *IEEE Transactions on Sustainable Energy*, vol. 1, no. 3, pp. 117–124, 2010.

[21] Y. Zhang, A. Lundblad, P. E. Campana, F. Benavente, and J. Yan, "Battery sizing and rule-based operation of grid-connected photovoltaic-battery system: A case study in Sweden," *Energy Conversion and Management*, vol. 133, pp. 249–263, 2017.

[22] T. Wakui, K. Sawada, R. Yokoyama, and H. Aki, "Predictive management for energy supply networks using photovoltaics, heat pumps, and battery by two-stage stochastic programming and rule-based control," *Energy*, vol. 179, pp. 1302–1319, 2019.

[23] D. M. Rosewater, D. A. Copp, T. A. Nguyen, R. H. Byrne, and S. Santoso, "Battery energy storage models for optimal control," *IEEE Access*, vol. 7, pp. 178 357–178 391, 2019.

[24] S. Zahmoun, A. Ouammi, R. Sacile, R. Benchrifa, and E. Zero, "Optimal operation scheduling of a combined wind-hydro system for peak load shaving," *IEEE Transactions on Automation Science and Engineering*, vol. 21, no. 4, pp. 7117–7130, 2024.

[25] P. Roy, J. He, and Y. Liao, "Optimal scheduling for dispatchable utility-scale solar PV power with battery-supercapacitor hybrid energy storage system," in *2022 IEEE Power & Energy Society General Meeting (PESGM)*. IEEE, 2022, pp. 1–5.

[26] M. Kaheni, A. V. Papadopoulos, E. Usai, and M. Franceschelli, "A privacy-preserving distributed greedy framework to desynchronize power consumption in a network of thermostatically controlled loads," *IEEE Transactions on Control Systems Technology*, vol. 32, no. 6, pp. 2476–2483, 2024.

[27] L. Jing, H. Zhao, S. Su, and W. Wei, "A fuzzy incremental proportional integral derivative control strategy for flywheel energy storage machines in autonomous vehicles," *IEEE Transactions on Automation Science and Engineering*, vol. 21, no. 3, pp. 2374–2386, 2024.

[28] M. Kaheni, E. Usai, and M. Franceschelli, "Resilient and privacy-preserving multi-agent optimization and control of a network of battery energy storage systems under attack," *IEEE Transactions on Automation Science and Engineering*, vol. 21, no. 4, pp. 5320–5332, 2024.

[29] Y. Li, D. M. Vilathgamuwa, D. E. Quevedo, C. F. Lee, and C. Zou, "Ensemble nonlinear model predictive control for residential solar battery energy management," *IEEE Transactions on Control Systems Technology*, vol. 31, no. 5, pp. 2188–2200, 2023.

[30] C. Liu, H. Ma, H. Zhang, X. Shi, and F. Shi, "A MILP-based battery degradation model for economic scheduling of power system," *IEEE Transactions on Sustainable Energy*, vol. 14, no. 2, pp. 1000–1009, 2023.

[31] H. Moring and J. L. Mathieu, "Scheduling battery energy storage systems under battery capacity degradation uncertainty," in *2022 American Control Conference (ACC)*. IEEE, 2022, pp. 5300–5307.

[32] A. Ouammi, Y. Achour, D. Zejli, and H. Dagdougui, "Supervisory model predictive control for optimal energy management of networked smart greenhouses integrated microgrid," *IEEE Transactions on Automation Science and Engineering*, vol. 17, no. 1, pp. 117–128, 2020.

[33] J. Fu, J. Åslund, and E. Uhlin, "A simulation framework for off-road transport operations using electric construction vehicles," in *2019 IEEE Intelligent Transportation Systems Conference (ITSC)*. IEEE, 2019, pp. 2539–2544.

[34] [Online]. Available: https://www.lythbattery.com/calb-l148n58a-3-7v-58ah-nmc-battery-cell/

[35] I. M. L. Pataro, J. D. Gil, M. V. Americano da Costa, L. Roca, J. L. Guzmán, and M. Berenguel, "A stochastic nonlinear predictive controller for solar collector fields under solar irradiance forecast uncertainties," *IEEE Transactions on Control Systems Technology*, vol. 32, no. 1, pp. 99–111, 2024.

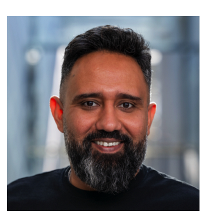

Mojtaba Kaheni (M'2023) is a Postdoctoral Researcher at the School of Innovation, Design, and Technology (IDT), Mälardalen University, Västerås, Sweden. He received his M.Sc. and Ph.D. in Control Engineering from Shahrood University of Technology, Shahrood, Iran, in 2011 and 2019, respectively. Dr. Kaheni has held visiting scholar positions at the University of Florence, Italy, and Lund University, Sweden. From August 2020 to December 2022, he served as a Postdoctoral Researcher at the University of Cagliari, Italy. His research interests include demand-side load management, distributed optimization, multi-agent systems, and resiliency.

Jiali Fu is a senior researcher at the Swedish National Road and Transport Research Institute (VTI), Stockholm, Sweden. She received the M.Sc. degree in Engineering Physics in 2010 and the Ph.D. degree in Transport Sciences in 2017 from KTH Royal Institute of Technology, Sweden. She worked as a post-doctoral researcher in the Department of Electrical Engineering, Linköping University, Sweden, during 2018–2020. Since April 2020, she has worked as a researcher at the Swedish National Road and Transport Research Institute (VTI). Her current research interests include application of mathematical modelling, and data-driven management and decision-support for transport systems.

Alessandro V. Papadopoulos (SM'19) is a Full Professor of Electrical and Computer Engineering at Mälardalen University, Västerås, Sweden, and a QUALIFICA Fellow at the University of Málaga, Spain. Since March 2024, he has been the scientific leader of Applied AI at Mälardalen University. He received his B.Sc. and M.Sc. (summa cum laude) degrees in Computer Engineering from the Politecnico di Milano, Milan, Italy, and his Ph.D. (Hons.) degree in Information Technology from the Politecnico di Milano, in 2013. He was a Postdoctoral researcher at the Department of Automatic Control, Lund, Sweden (2014-2016) and Politecnico di Milano, Milan, Italy (2016). He was the Program Chair for the Mediterranean Control Conference (MED) 2022, the Euromicro Conference on Real-Time Systems (ECRTS) 2023, and the ACM/SPEC International Conference on Performance Engineering (ICPE) 2025. He is an associate editor for the ACM Transactions on Autonomous and Adaptive Systems, Control Engineering Practice, and Leibniz Transactions on Embedded Systems. His research interests include robotics, control theory, real-time systems, and autonomic computing.